The Journal of Physical Chemistry A

 VOLUME 102, NUMBER 1, JANUARY 1, 1998

ARTICLES

Kinetics and Thermochemistry of the Reversible Combination Reaction of the Phenoxy Radical with NO

Florence Berho, Françoise Caralp, Marie-Thérèse Rayez, and Robert Lesclaux*

Laboratoire de Physico-Chimie Moléculaire, Université Bordeaux I, UMR 5803 CNRS, 33405 Talence Cedex, France

Emil Ratajczak

Department of Physical Chemistry, Wroclaw University of Medicine, Pl. Nankiera 1, 50-140 Wroclaw, Poland

Received: August 7, 1997; In Final Form: October 22, 1997[⊗]

The kinetics of the association reaction of the phenoxy radical with NO were investigated using a flash photolysis technique coupled to UV absorption spectrometry. This yielded $k(C_6H_5O + NO) = (1.65 \pm 0.10) \times 10^{-12}$ cm^3 molecule^{-1} s^{-1}, with no significant temperature effect over the temperature range 280−328 K. Experiments were performed at atmospheric pressure, and theoretical calculations using the RRKM method showed that the rate constant is at the high-pressure limit above ≈50 Torr for temperatures below 400 K. Upon increasing the temperature, the reaction was found to be reversible, and the equilibrium kinetics have been studied at seven temperatures between 310 and 423 K. The equilibrium constant can be expressed as $\ln(K_c/\text{cm}^3\ \text{molecule}^{-1}) = -(63.3 \pm 1.0) + (10\,140 \pm 1000)\text{K}/T$. Thermodynamic treatment of the data by the Third Law method of analysis yielded $\Delta H°_{298} = (-87.3 \pm 8.0)$ kJ mol^{-1} (yielding $\Delta H°_0 = (-83.8 \pm 8.0)$ kJ mol^{-1} and $\Delta H°_{f,298}(C_6H_5O(NO)) = (51.5 \pm 8.0)$ kJ mol^{-1}), corresponding to the calculated $\Delta S°_{298} = (-164.9 \pm 8.0)$ J mol^{-1} K^{-1}. All spectroscopic parameters necessary for RRKM calculations and for the entropy determination using statistical thermodynamics were calculated using both semiempirical (MNDO) and DFT methods. Influence of the resonance stabilization energy of radicals on R−NO bond dissociation energy is discussed.

Introduction

The oxidation of aromatic hydrocarbons in the gas phase is now becoming a topical issue, as such compounds are extensively used as additives in lead-free gasoline because of their high octane value. Nevertheless, few kinetic data are available concerning the reactions of the phenoxy radical (C_6H_5O), which is a key intermediate in the oxidation of small aromatic compounds. For instance, the high-temperature oxidation of benzene initiated by reaction with atoms (O or H) or radicals (OH or CH_3) yields the phenyl radical C_6H_5, which can react with molecular oxygen, forming the phenoxy radical and initiating a chain reaction through O atom production.[1] The phenoxy radical is also an intermediate in the oxidation of other aromatic compounds, such as phenol and benzaldehyde. Therefore, kinetic data are necessary for better understanding and modeling of the oxidation processes of aromatic hydrocarbons.

Studies of association reactions with hydrogen atoms[1,2] and methyl radicals[3,4] (yielding phenol and anisole or cresols, respectively) have been reported. Concerning the association reaction with NO, only one combined experimental and theoretical study has been performed.[5] In the present work, the equilibrated reaction between C_6H_5O and NO has been investigated above 310 K.

* Corresponding author. E-mail: lesclaux@cribx1.u-bordeaux.fr.
[⊗] Abstract published in *Advance ACS Abstracts*, December 1, 1997.

S1089-5639(97)02576-0 CCC: $15.00
Published on Web 01/01/1998

$$C_6H_5O + NO + M \rightleftarrows C_6H_5O(NO) + M \quad (1, -1)$$

The results were obtained from kinetic simulations of phenoxy radical decay traces recorded using the flash photolysis technique. The equilibrium constant was determined as a function of temperature, from 310 to 423 K, to derive the thermochemical parameters, the enthalpy and entropy changes, for reaction 1. These values were obtained using both Second and Third Law thermodynamic analysis. Quantum calculations were used for the determination of structural parameters of C_6H_5O and C_6H_5O-(NO), including the three possible isomers of $C_6H_5O(NO)$ resulting from the resonant structure of the phenoxy radical.

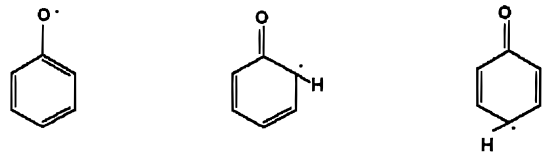

a **b** **c**

In addition, kinetic studies were performed on the association of phenoxy radicals with NO at lower temperatures ($T = 280-328$ K, $P = 760$ Torr, M = N_2), where the association and dissociation components of the decay could be separated during the approach to equilibrium. The kinetics of the phenoxy self-reaction, which are necessary to fully characterize the chemical system at low NO concentrations and when reaction 1 is equilibrated, are reported separately.[6]

Experimental Section

All experiments were performed using the flash photolysis technique, coupled to UV absorption spectrometry, to monitor radical concentrations in real time. This technique has been described in detail previously[7] and can be briefly summarized as follows.

Phenoxy radicals were produced by flash photolysis of Cl_2/phenol/N_2 mixtures

$$Cl_2 + h\nu \rightarrow 2Cl \quad (2)$$

$$Cl + C_6H_5OH \rightarrow HCl + C_6H_5O \quad (3)$$

with $k_3 = 2.4 \times 10^{-10}$ cm^3 molecule^{-1} s^{-1}.[1] Recently, this reaction has been shown to be a clean source of phenoxy radicals.[1]

All experiments were performed at atmospheric pressure (760 ± 10 Torr) and in the temperature range 280−423 K. The desired temperature was controlled to within ±3 K by either flowing thermostated water in an outer jacket surrounding the cylindrical reaction cell (4 cm i.d., 70 cm length) or by heating in an oven for temperatures above 370 K.

The photolyzing light was provided by an argon flash lamp. A Pyrex tube was used to filter out radiation of $\lambda < 280$ nm in order to prevent any photodissociation of phenol during the flash. Gas mixtures were prepared using calibrated flow controllers, and the total gas flow was adjusted so that the reaction cell was replenished between each flash to prevent any secondary photodissociation of reaction products.

Phenoxy radical concentrations were monitored by UV absorption spectrometry at $\lambda = 240$ nm. According to the phenoxy UV spectrum determined previously,[6] this wavelength appeared to be the most appropriate for kinetic studies by providing good signal-to-noise ratios and low residual absorption due to reaction products. The analysis beam, generated by a deuterium lamp, passed once through the cell and was then directed onto a monochromator (2 nm resolution)/photomultiplier unit. The signal was then digitized and transferred to a computer for averaging and further data analysis. Kinetic simulations were performed by numerical integration and fitted to the averaged decay traces using nonlinear least-squares analysis.

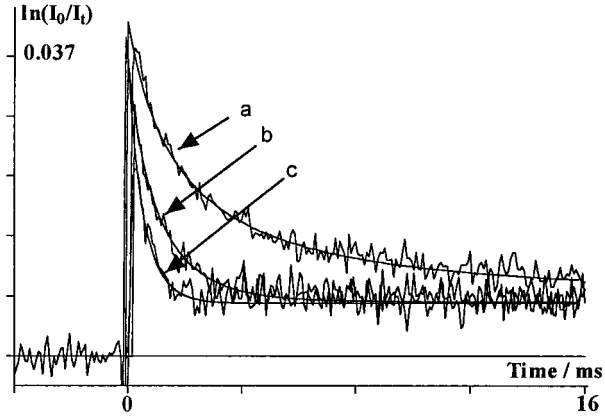

Figure 1. Typical decay traces recorded at 240 nm following the flash photolysis of Cl_2/phenol/NO/N_2 mixtures at room temperature and atmospheric pressure: (a) absence of NO; (b) [NO] = 3.3×10^{14} molecule cm^{-3}; (c) [NO] = 8.2×10^{14} molecule cm^{-3} The solid lines are simulations of the data.

To introduce phenol in the gas mixture, nitrogen was slowly flowed through a glass tube whose walls were coated with solid phenol. The phenol concentration was monitored by its absorption at $\lambda = 275$ nm ($\sigma = 6.20 \times 10^{-18}$ cm^2 molecule^{-1})[6] and that of molecular chlorine at $\lambda = 330$ nm ($\sigma = 2.56 \times 10^{-19}$ cm^2 molecule^{-1}).[8] Concentrations were adjusted such that the conversion of chlorine atoms into phenoxy radicals was total and very fast (5−20 μs) compared to the phenoxy reaction time (>10 ms). Typically, concentrations of reactants were (units of molecule cm^{-3}): [phenol] = $(2-6) \times 10^{14}$, [Cl_2] = $(3-9) \times 10^{15}$, [NO] = $(0.7-15) \times 10^{14}$, resulting in initial radical concentrations of $(0.3-2) \times 10^{13}$ molecule cm^{-3}.

Nitrogen (AGA Gaz Spéciaux, purity > 99.995%), oxygen (AGA Gaz Spéciaux, purity > 99.995%), phenol (Aldrich, 99+%), molecular chlorine (Messer, 5% in N_2, purity > 99.9%), and nitric oxide (AGA Gaz Spéciaux, 0.96% in N_2, purity > 99.9%) were used without further purification.

Results

Decay traces corresponding to the phenoxy radical self-reaction were recorded at 240 nm and at each temperature investigated, both to measure the initial radical concentration, using the previously determined UV absorption cross sections,[6] and to characterize the chemical system in the absence of NO (Figure 1a).

The study of the phenoxy radical self-reaction is reported in a separate publication.[6] The system was analyzed using the following simple reaction mechanism:

$$Cl + C_6H_5OH \rightarrow HCl + C_6H_5O \quad (3)$$

$$2C_6H_5O \rightarrow \text{product} \quad (4)$$

$$C_6H_5O + Cl_2 \rightarrow C_6H_5O(Cl) + Cl \quad (5)$$

The product of reaction 4 is probably a dimer that rearranges to give dihydroxybiphenyl isomers.[9] The product of reaction

TABLE 1: Reaction Mechanism and Parameters Used in Simulations of Decay Traces Recorded at 240 nm (P = 760 Torr, M = N_2)

reaction	k/cm^3 molecule^{-1} s^{-1}	ref
$Cl_2 + h\nu \rightarrow 2Cl$		
$Cl + C_6H_5OH \rightarrow HCl + C_6H_5O$	2.4×10^{-10}	(1)
$C_6H_5O + C_6H_5O \rightarrow$ products	$(1.44 \pm 0.16) \times 10^{-10} \exp[(631 \pm 37)\text{K}/T]$	(6)
$C_6H_5O + Cl_2 \rightarrow C_6H_5O(Cl) + Cl$	1×10^{-14} [a]	(6)
$C_6H_5O + NO \rightarrow C_6H_5O(NO)$	$(1.65 \pm 0.1) \times 10^{-12}$	(this work)
$C_6H_5O(NO) \rightarrow C_6H_5O + NO$	k_{-1} [b]	(this work)
$Cl + NO + M \rightarrow ClNO + M$	$k(T) = 6.07 \times 10^{-6} \times T^{-2.6}$ at 760 Torr	(8)
$C_6H_5O + C_6H_5O(NO) \rightarrow$ products	4.5×10^{-12} [a]	(this work)

absorption cross sections

$\sigma(C_6H_5O) = 2.55 \times 10^{-17}$ cm^2 molecule^{-1}
$\sigma(C_6H_5O(NO)) = 5.0 \times 10^{-18}$ cm^2 molecule^{-1}
$\sigma(C_6H_5OH) = 5.0 \times 10^{-19}$ cm^2 molecule^{-1}
$\sigma(Cl_2)$ is negligible at 240 nm

[a] No significant variation with T could be detected in the temperature range investigated. [b] $k_{-1} = k_1/K_c$, with $\ln(K_c/\text{cm}^3\ \text{molecule}^{-1}) = -(63.3 \pm 1.0) + [(10\ 140 \pm 1000)\text{K}/T]$ (this work).

5, $C_6H_5O(Cl)$, represents the three possible isomers corresponding to the three resonance structures of the phenoxy radical.

The values of the parameters used in simulations are listed in Table 1. It must be stressed that the absorption cross section values assigned to the products of reactions 4 and 5 to characterize the residual absorption have no individual meaning, as they strongly depend on the value assigned to k_5, which bears a large uncertainty factor of about 3.[6] Nevertheless it was shown that those parameters, characterizing the residual absorption, were of negligible importance in the determination of the kinetic parameters and equilibrium constant of reaction 1.

A. Kinetics of the Association Reaction 1.

$$C_6H_5O + NO + M \rightarrow C_6H_5O(NO) + M \qquad (1)$$

Decay traces were recorded by photolyzing Cl_2/phenol/NO mixtures, diluted in nitrogen as carrier gas, at 760 Torr and in the temperature range 280−328 K. In the presence of NO, the phenoxy decay rate was significantly increased (Figure 1b,c), compared to the decay rate observed in the absence of NO (Figure 1a). All experiments were performed under pseudo-first-order conditions, using an excess of NO. The concentration of NO was varied over the range $(0.7-3.5) \times 10^{14}$ molecule cm^{-3}, which resulted in pseudo-first-order rate constants varying by a factor of about 5 at each temperature.

Simulations of decay traces were performed using a reaction mechanism that included reaction 1, between C_6H_5O and NO, in addition to reactions 3−5, which characterized the chemical system in the absence of NO (Table 1). The pseudo-first-order rate constant, $k^I = k_1[NO]$, was optimized for each concentration of NO, and the value of k_1 was obtained from the plot of k^I against [NO]. The plot resulted in a straight line passing through the origin, within experimental uncertainties, showing that experimental conditions were appropriate (Figure 2). The rate constant k_1 was derived from the slope of the straight lines obtained at each temperature investigated. The results are reported in Table 2, along with the statistical uncertainties.

A slight decrease of the rate constant is observed upon increasing the temperature, resulting in the following rate expression:

$$k_1 = (1.70 \pm 0.1) \times 10^{-12}(T/298)^{-(0.79\pm0.20)}\ \text{cm}^3\ \text{molecule}^{-1}\ \text{s}^{-1} \quad (280 < T < 328\ \text{K})$$

However, the observed variation of k_1 with temperature is of the order of the magnitude of experimental uncertainties and thus is not significant. Consequently, the proposed value of k_1 for the temperature range investigated is the average of the values given in Table 2:

$$k_1 = (1.65 \pm 0.1) \times 10^{-12}\ \text{cm}^3\ \text{molecule}^{-1}\ \text{s}^{-1}$$

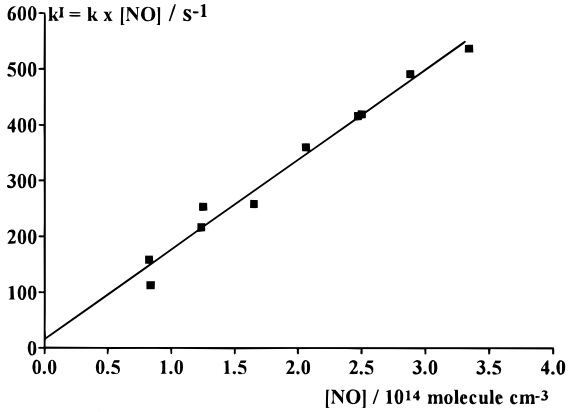

Figure 2. Plot of the measured pseudo-first-order rate constant $k^I = k_1[NO]$ against NO concentration, derived from experimental data collected at room temperature and atmospheric pressure.

TABLE 2: Temperature Dependence of k_1

T/K	$k_1/10^{-12}$ cm^3 molecule^{-1} s^{-1}	no. of expts
280	1.76 ± 0.10	10
293	1.70 ± 0.10	10
310	1.67 ± 0.05	9
328	1.54 ± 0.20	10

Measurements of k_1 could only be performed at temperatures lower than 330 K. At 280 and 293 K, only k_1 was necessary to properly simulate the decay traces, whereas at 310, 320, and 328 K the occurrence of the equilibrium could not be ignored. The value of k_{-1} had to be included in the reaction mechanism for an accurate analysis of decay traces. At higher temperatures, k_1 could no longer be measured because decay rates became too fast as higher concentrations of NO had to be used to prevent the equilibrium from being shifted toward the reactants. As explained below, only the ratio k_1/k_{-1} could be used in the determination of the equilibrium constant.

A pressure effect can be expected for association processes with low reaction enthalpy such as reaction 1, as shown below. To estimate if any pressure effect could be observed in the pressure range covered by our experimental setup (30−760 Torr), the pressure dependence of k_1 was estimated using RRKM

TABLE 3: Molecular Parameters for the Phenoxy Radical and (C_6H_5O(NO) Isomers

Vibrational Frequencies (cm^{-1})

NO:	1992
phenoxy:	195, 380, 444, 485, 531, 598, 657, 795, 806, 811, 921, 973, 986, 994, 1018, 1098, 1175, 1176, 1289, 1353, 1433, 1458, 1498, 1565, 1604, 3192, 3199, 3214, 3224, 3227
(C_6H_5O(NO) isomer **1**:	69, 133, 160, 293, 362, 423, 465, 536, 608, 635, 704, 751, 791, 844, 904, 932, 965, 992, 1020, 1053, 1108, 1191, 1198, 1246, 1345, 1363, 1503, 1536, 1649, 1654, 1804, 3189, 3198, 3210, 3221, 3223
(C_6H_5O(NO) isomer **2**:	27, 62, 172, 273, 342, 405, 455, 489, 518, 573, 607, 739, 761, 799, 881, 967, 986, 993, 1020, 1031, 1163, 1192, 1207, 1246, 1321, 1406, 1453, 1599, 1679, 1708, 1765, 3136, 3180, 3189, 3207, 3216
(C_6H_5O(NO) isomer **3**:	33, 49, 194, 278, 333, 419, 457, 464, 540, 578, 610, 772, 777, 794, 871, 935, 987, 1011, 1021, 1033, 1159, 1192, 1225, 1272, 1370, 1416, 1419, 1661, 1672, 1708, 1761, 3083, 3178, 3179, 3209, 3210

Rotational Constants (cm^{-1})

NO	1.6805		
C_6H_5O	0.1836	0.0926	0.0616
C_6H_5O(NO) isomer **1**	0.1655	0.0328	0.0280
C_6H_5O(NO) isomer **2**	0.0829	0.0543	0.0376
C_6H_5O(NO) isomer **3**	0.1389	0.0358	0.0312

Parameters Used in RRKM Calculations

$\Delta H°_0 = (-83.8 \pm 8.0)$ kJ mol^{-1} (this work)

Lennard-Jones Parameters

	N_2	C_6H_5O(NO)
σ (Å)	3.68	5.0
ϵ/k	91.5	400

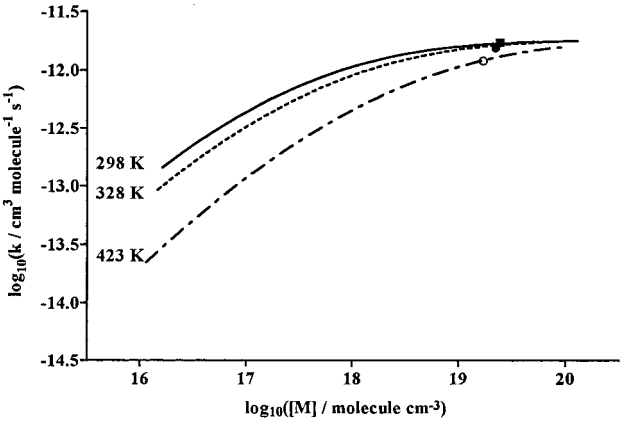

Figure 3. Falloff curves for the reaction $C_6H_5O + NO + M \rightarrow C_6H_5O$(NO) + M resulting from RRKM calculations performed at different temperatures. ■, ●, experimental data (this work); ○, calculated data.[5]

calculations at 298, 328, and 423 K. The parameters necessary to perform calculations ($\Delta H°_0$, structural parameters) were determined as explained in the next section and given in Table 3. The falloff curves calculated at each temperature are represented in Figure 3, using $\beta_c = 0.2$ and $k_\infty = 1.8 \times 10^{-12}$ cm^3 $molecule^{-1}$ s^{-1}, independent of temperature. On the basis of these results, it can be concluded that any pressure dependence would be too small to be experimentally observable in the pressure range considered, whatever the temperature, below 423 K. As a consequence, no experiments were performed at pressures lower than 760 Torr, and it is concluded that the reported values of k_1 correspond to the high-pressure limit.

B. Equilibrium and Thermodynamics of the Reaction System 1, −1. *1. Experimental Determination of the Equilibrium Constant.*

$$C_6H_5O + NO + M \rightleftarrows C_6H_5O(NO) + M \quad (1, -1)$$

As stated above, at temperatures higher than 310 K, decay traces could not be simulated without taking into account the dissociation of C_6H_5O(NO) (reaction −1). The experimental decay traces began to exhibit kinetic profiles indicative of the establishment of an equilibrium (Figure 4b). Two regimes

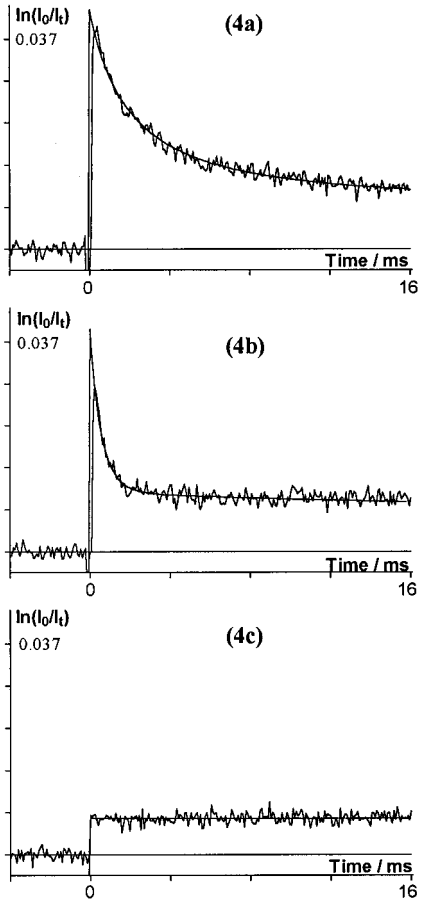

Figure 4. Typical decay traces recorded at 240 nm following the flash photolysis of Cl_2/phenol/NO/N_2 mixtures at 328 K and atmospheric pressure: (a) absence of NO; (b) [NO] = 6.92×10^{14} molecule cm^{-3}; (c) [NO] = 1.54×10^{16} molecule cm^{-3}. The solid lines are simulations of the data.

became apparent, the first one dominated by the rapid association of phenoxy radicals with NO and the second one corresponding to the absorption signal resulting from the establishment of the phenoxy radical and C_6H_5O(NO) concentrations at equilibrium. Upon increasing the temperature toward the upper

TABLE 4: Temperature Dependence of the Equilibrium Constant for Reactions 1, −1

T/K	[NO]/10^{15} molecule cm^{-3}	K_c/cm^3 molecule^{-1}	K_p/atm^{-1}	no. of expts
310	0.12−0.71	$(2.74 \pm 0.90) \times 10^{-14}$	$(6.48 \pm 2.20) \times 105$	9
320	0.11−0.70	$(1.47 \pm 1.20) \times 10^{-14}$	$(3.36 \pm 2.70) \times 105$	10
328	0.07−0.30	$(1.18 \pm 0.35) \times 10^{-14}$	$(2.65 \pm 0.80) \times 105$	7
347	0.14−0.67	$(1.78 \pm 0.48) \times 10^{-15}$	$(3.76 \pm 1.01) \times 104$	10
370	0.33−0.46	$(3.22 \pm 0.97) \times 10^{-16}$	$(6.40 \pm 1.90) \times 103$	8
403	3.0−9.4	$(3.65 \pm 1.00) \times 10^{-17}$	$(6.64 \pm 1.00) \times 102$	10
423	10.0−34.7	$(1.10 \pm 0.33) \times 10^{-17}$	$(1.89 \pm 0.58) \times 102$	7

limit, large concentrations of NO had to be used and the first part of the signal described above became so fast that it could not be observed anymore. Thus, only the postequilibrium part of the decay signal could be recorded.

Using a large excess of NO, a residual absorption was observed (Figure 4c), indicating that the absorption of the adduct had to be taken into account when simulating decay traces. This residual absorption was used to estimate the absorption cross section of the adduct: $\sigma(C_6H_5O(NO)) = 5.0 \times 10^{-18}$ cm^2 molecule^{-1} at 240 nm. No significant variation of this value could be observed when changing the temperature. The excess of NO had to be large enough to ensure that the equilibrium was completely shifted toward the formation of the adduct $C_6H_5O(NO)$. However, at such high NO concentrations, the reaction of chlorine atoms with NO

$$Cl + NO + M \rightarrow ClNO + M \qquad (6)$$

had to be taken into account as it competes with the reaction of Cl atoms with phenol, forming phenoxy radicals. Omitting reaction 6 in simulations would have resulted in overestimating the initial radical concentration of phenoxy radicals. The occurrence of reaction 6 was most significant at the highest temperatures investigated, where high NO concentrations had to be used (Table 4) and resulted in up to 20% of chlorine atom loss.

The equilibrium constant was obtained by measuring the ratio of the association and dissociation rate coefficients ($K_c = k_1/k_{-1}$). At the lower end of our temperature range ($T < 330$ K), where NO concentrations were low, decay traces included the association step (Figure 4b) and simulations consisted of optimizing both k_1 and k_{-1} as individual parameters. At higher temperatures, where NO concentrations were high, the association step became too fast and simulations consisted of optimizing the ratio k_1/k_{-1} directly.

The postequilibrium decay of the signal was found to be slightly faster than that calculated by only considering the phenoxy radical self-reaction. A loss other than radical recombination was clearly increasing the phenoxy decay rate, either directly or indirectly through adduct removal. A similar behavior of the postequilibrium signal has already been observed in previous studies of association reactions with NO.[10] A reaction of the phenoxy radical with the adduct $C_6H_5O(NO)$ was considered to be representative of this additional chemistry:

$$C_6H_5O + C_6H_5O(NO) \rightarrow \text{products} \qquad (7)$$

This reaction was added to the reaction mechanism, and adjusting its rate constant to fit the post-equilibrium decay yielded: $k_7 \approx 4.5 \times 10^{-12}$ cm^3 molecule^{-1} s^{-1}, with no clear temperature dependence. It must be emphasized that such a reaction is always too slow to perturb the equilibrium and hence to affect any determination of the equilibrium constant. Possible products of reaction 7 are a phenoxy dimer and NO, but we have no evidence for the formation of such products.

The equilibrium constant was measured between 310 and 423 K for 7−10 different concentrations of NO at each temperature. The results are given in Table 4, along with the experimental conditions.

2. Quantum Calculations. The thermochemical parameters of reaction 1, enthalpy and entropy changes, can be derived from the above experimental determination of the temperature dependence of the equilibrium constant, using either the Second or Third Law thermodynamic analysis. The former only requires experimental data whereas the latter also requires the calculated value of the entropy change of reaction 1. Both methods were used in this work, and the results are reported below. All spectroscopic and structural parameters necessary to calculate the entropy change of reaction 1 were derived from quantum calculations.

The entropy was calculated for each species involved in the reaction, even though the NO and C_6H_5O entropy values can be easily determined. Nevertheless, they were calculated using the same method as for $C_6H_5O(NO)$, expecting the errors to cancel to some extent when calculating ΔS. The $C_6H_5O(NO)$ species has three isomers

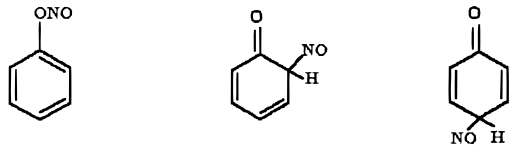

1 **2** **3**

resulting from the combination of NO with either the benzenoid structure **a** (giving isomer **1**) or quinoid structures **b** and **c** (giving isomers **2** and **3**) of the phenoxy radical. Furthermore, each isomer can undergo subsequent rearrangements to yield the following three compounds:

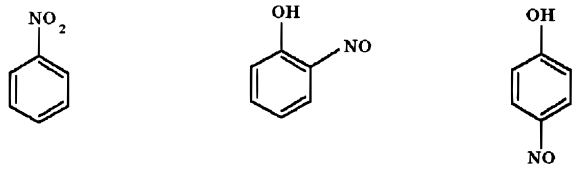

4 **5** **6**

However, it is likely that such internal rearrangements, which require significant activation energy, would not take place during the reaction time scales of interest in this work. In addition, they must be irreversible as the above products are more stable than the $C_6H_5O(NO)$ isomers. Consequently, they cannot be involved in the equilibrium, and the entropy was only calculated for the $C_6H_5O(NO)$ isomers **1**, **2**, and **3**. It should be noted that if the above rearrangements were to occur at a rate significantly high to perturb the equilibrium, the postequilibrium decay would have been much faster than that actually observed.

Quantum calculations were performed using density functional theory (DFT), with Becke's three-parameter function[11] and the nonlocal correlation provided by the LYP expression (B3LYP).[12] This method is implemented in the Gaussian94 computational package.[13] The double-ζ 6-31G(d) basis set including the polarization function has been used. This choice was made as this method is known to give reliable structures, vibrational frequencies, and energies for stable systems. The calculated vibrational frequencies, for nitric oxide, the phenoxy

TABLE 5: Calculated Entropies Using DFT and MNDO Methods and Calculated $\Delta S°_{298}$ for Reaction 1

	DFT $S°_{298}$ (J mol^{-1} K^{-1})	MNDO $S°_{298}$ (J mol^{-1} K^{-1})
NO	210.5	210.0
C_6H_5O	314.8	318.0
C_6H_5O(NO) 1	360.4	366.0
C_6H_5O(NO) 2	377.0	369.0
C_6H_5O(NO) 3	376.5	370.0
$\Delta S°_{298}$ (J mol^{-1} K^{-1})[a]	−164.9	−162.0

[a] Calculated for isomer 1.

radical and the three isomers are reported in Table 3. They agree satisfactorily with those already reported and calculated using other methods.[14−16] For the phenoxy radical, our theoretical results for the vibrational frequencies are in good agreement with the experimental data available to date.[17,18] The values of $S°_{298}$ derived from these optimized molecular structures are given in Table 5. They were confirmed using the MNDO semiempirical method,[19] combined with the gradient minimization algorithm AMPAC[20] (also reported in Table 5).

In addition, DFT results confirmed previous calculations (using ab initio MP4(SDQ)/6-31G(d)//HF and isodesmic corrections),[5] showing that isomer **1** is more stable than isomers **2** and **3** by about 30 kJ mol^{-1}. This led us to consider that only the reaction forming isomer **1** should be taken into account in the determination of the equilibrium parameters. Thus, $\Delta S°_{298}$ was calculated using the entropy of isomer **1** (which is not significantly different from the entropy of other isomers), giving for reaction 1:

$$\Delta S°_{298} = -(164.9 \pm 8.0) \text{ J mol}^{-1} \text{ K}^{-1}$$

Errors were estimated from uncertainties in parameters used in calculations and, in particular, on the lowest vibrational frequencies.

Note that the calculated value is consistent with other theoretical and experimental similar determinations of $\Delta S°_{298}$ concerning the association reactions of the allyl and benzyl radicals with NO, (−154.0 ± 9.0) and (−159.0 ± 9.0) J mol^{-1} K^{-1} respectively.[10] As the similar bond (RO−NO) is formed in the reaction, a value close to that found here for reaction 1 can be reasonably expected.

3. Thermochemical Parameters of Reaction 1. The enthalpy and entropy change of reaction 1 were first determined by a Second Law analysis by plotting the experimental values of ln K_p, listed in Table 4, against $1/T$ (Van't Hoff plot) as shown in Figure 5a (dashed line). The slope and intercept of a linear regression analysis yielded

$$\Delta H°_{298} = -(80.8 \pm 3.0) \text{ kJ mol}^{-1}$$

$$\text{and} \quad \Delta S°_{298} = -(146.3 \pm 8.0) \text{ J mol}^{-1} \text{ K}^{-1} \quad (\text{errors } 1\sigma)$$

Considering the possible errors on K_c measurements (see Discussion below), we estimate that overall uncertainties in the experimental (Second Law) ΔH and ΔS values are 8.0 kJ mol^{-1} and 20.0 J mol^{-1} K^{-1}, respectively. The corrections that were applied to derive $\Delta H°_{298}$ and $\Delta S°_{298}$ by taking into account their variation with temperature were found to be smaller than 1% over the temperature range of interest (310−423 K). This was expected as the temperature range investigated was not much above room temperature.

As the equilibrium constant was determined over a narrow temperature range, the accuracy of these results is questionable.

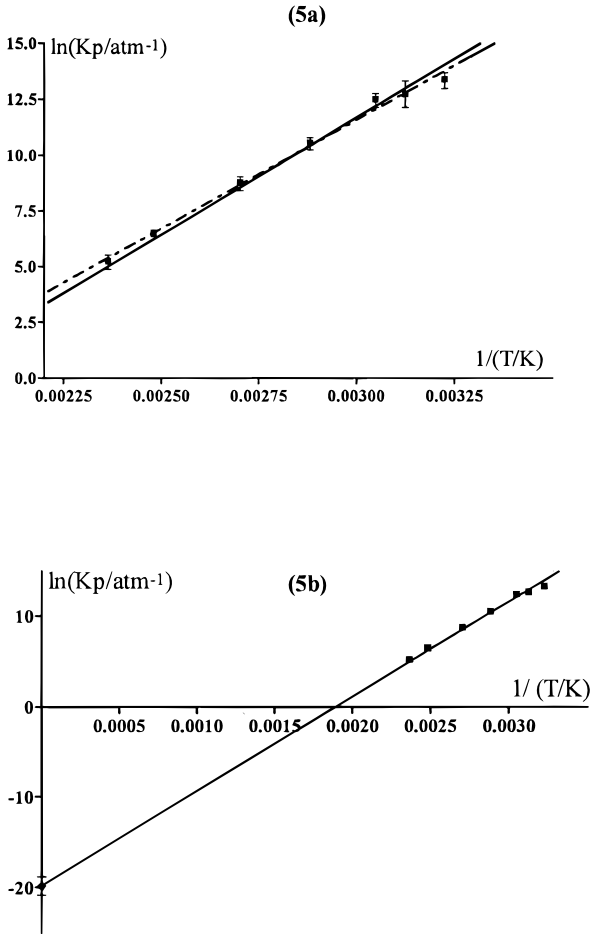

Figure 5. Van't Hoff plots for the equilibrated reaction 1: dashed line, Second Law analysis; solid line, Third Law analysis.

A better accuracy is generally provided by the Third Law method, which consists of calculating the value of $\Delta S°_{298}$ using statistical thermodynamics, as detailed above, and deriving $\Delta H°_{298}$ from the experimental values of the equilibrium constant. $\Delta H°_{298}$ was thus determined from a linear least-squares analysis, this time constrained to pass through the calculated value of $\Delta S°_{298}$ (Figure 5b). This method yields $\Delta H°_{298} = -(87.3 \pm 3.0)$ kJ mol^{-1} for $\Delta S°_{298} = -(164.9 \pm 8.0)$ J mol^{-1} K^{-1}, the errors being estimated by combining the uncertainty in the calculated $\Delta S°_{298}$ value and the experimental uncertainty (1σ) in the equilibrium constant. In this case, possible errors on K_c measurements result in an overall uncertainty on the Third Law ΔH value of 8.0 kJ mol^{-1}.

A noticeable difference is observed between the values of $\Delta H°_{298}$ determined by the Second and Third Law analysis, (−80.8 ± 8.0) and (−87.3 ± 8.0) kJ mol^{-1}, respectively, but it can be considered that the two values agree within experimental and calculated uncertainties. In particular, in the case of the Second Law analysis, the temperature range explored for measurements of the equilibrium constant is too narrow to result in good accuracy in the value of ΔH determined. This is well illustrated by ignoring the K_p values obtained at the lowest temperatures (310 and 320 K), where the accuracy is the poorest (due to the low dissociation rate of C_6H_5O(NO)). Indeed, omitting these two measurements, the "second law values" are in very good agreement with the "third law values". It should be stressed, in addition, that the difference observed between the experimental and calculated ΔS ($\cong$ 18.6 J mol^{-1} K^{-1}) is much larger than the possible error on the calculated value (estimated to be less than 8.0 J mol^{-1} K^{-1}). The only way to

fit the calculated ΔS value to the experimental one would be to assign an unrealistic degree of looseness to the torsion modes in $C_6H_5O(NO)$. This indicates that the "second law value" derived from all measurements is indeed too small.

This allows us to conclude that the Third Law analysis gives the more reliable results. Thus, our recommended values of $\Delta H°_{298}$ and $\Delta S°_{298}$ are

$$\Delta H°_{298} = -(87.3 \pm 8.0) \text{ kJ mol}^{-1}$$

$$\text{and} \quad \Delta S°_{298} = -(164.9 \pm 8.0) \text{ J mol}^{-1} \text{ K}^{-1}$$

The corresponding Van't Hoff plot is represented by the solid line in Figure 5a,b. Note that it still fits the experimental data quite satisfactorily. The variation of K_c, derived from the above recommended parameters, can be expressed as:

$$\ln(K_c/\text{cm}^3 \text{ molecule}^{-1}) = -(63.3 \pm 1.0) + [(10\,140 \pm 1000)\text{K}/T]$$

The enthalpy of formation of $C_6H_5O(NO)$ at 298 K could also be estimated using our $\Delta H°_{298}$ value and those of NO and C_6H_5O (90.8 and 48.0 kJ mol^{-1} respectively[21−23])

$$\Delta H°_{f,298}(C_6H_5O(NO)) = 51.5 \pm 8.0 \text{ kJ mol}^{-1}$$

the most likely structure of $C_6H_5O(NO)$ being that of isomer **1**, as explained above.

$\Delta H°_0$ for reaction **1** could also be estimated at -83.8 ± 8.0 kJ mol^{-1} using $\Delta H°_{298}$ and the structural parameters given in Table 3. This value of $\Delta H°_0$ was used in the RRKM calculations reported above.

Discussion

The experimental work reported in this paper was focused on the determination of the rate constant and equilibrium constant of the association reaction of the phenoxy radical with NO. The mean rate constant found in the temperature range 280−328 K, $k_1 = (1.65 \pm 0.1) \times 10^{-12}$ cm^3 molecule^{-1} s^{-1}, is in good agreement with the recent determination of Yu et al. of $k_1 = 1.45 \times 10^{-12}$ cm^3 molecule^{-1} s^{-1} at room temperature.[5] It should be noted that this value is significantly lower than the rate constant values generally observed for radical combination reactions with NO, $(1-2) \times 10^{-11}$ cm^3 molecule^{-1} s^{-1} for both R- and RO-type radicals.[24] This particular behavior of the C_6H_5O + NO reaction can be related to its smaller enthalpy change compared to that of similar reactions of alkyl and alkoxy radicals, these being generally 70−80 kJ mol^{-1} higher. A similar trend was observed in the case of the benzyl and allyl radicals, which are also resonance stabilized, resulting in smaller enthalpy changes for their association reactions with NO, of -123 ± 5 kJ mol^{-1} and -110 ± 5 kJ mol^{-1} respectively.[10] The corresponding rate constants were found to be 9×10^{-12} and 7×10^{-12} cm^3 molecule^{-1} s^{-1} respectively.[10] The question of the resonance stabilization of these radicals is discussed below.

The rate constant k_1 was found to decrease slightly upon increasing temperature, with a $T^{-0.79}$ temperature dependence. However, as stressed above, the temperature range investigated is too narrow to expect an accurate determination of such a weak temperature dependence, which may be accounted for by uncertainties. This has led us to only report the average value of k_1 in the temperature range investigated. Nevertheless, the temperature dependence found in this work is quite close to that reported by Yu et al.[5] ($T^{-0.61}$ from 293 to 373 K).

According to the RRKM calculations, the rate constant reported for k_1 corresponds to the high-pressure limit. However, at pressures lower than 50 Torr, the reaction is definitely in the falloff region and the pressure dependence of k_1 must be taken into account, particularly upon increasing the temperature above room temperature.

The equilibrium constant was measured as a function of temperature with an accuracy that could not be better than 30% as estimated from the scatter of results (Table 4). The accuracy was the poorest at the lowest temperatures of this study where the reverse rate constant became too low and thus of reduced importance in simulations. This has led us to conclude that the Second Law method could not yield sufficient accuracy for the ΔH determination and only a Third Law analysis could yield reliable results.

Possible systematic errors on the equilibrium constant would arise from errors on the parameters used in simulations. Some of these parameters, $\sigma(C_6H_5O)$, $\sigma(C_6H_5OH)$, $\sigma(C_6H_5OCl)$, the rate constant and product absorption cross section of the $C_6H_5O + C_6H_5O$ reaction, are those used to fit the decay traces recorded in the absence of NO and their associated uncertainties should not introduce significant errors. The same situation should prevail for $\sigma(C_6H_5O(NO))$ which is determined in the presence of a large excess of NO. However, under such conditions, the loss of chlorine atoms by reaction with NO cannot be taken into account accurately, thus introducing an uncertainty in $\sigma(C_6H_5O(NO))$. It was estimated that this error was minor compared to the 30% statistical uncertainty on K_c measurements at each temperature. As mentioned above, no significant error could result from the occurrence of the reaction between C_6H_5O and $C_6H_5O(NO)$ and from the slow isomerization of $C_6H_5O(NO)$.

As already stressed, the determination of the thermochemical parameters, using the Second Law method of analysis, is of poor accuracy. Nevertheless, it is shown that the most accurate values of the equilibrium constant yield a $\Delta H°_{298}$ value in quite good agreement with the Third Law analysis. Thus we have considered the Third Law values as being of greater accuracy compared to those obtained by the Second Law method, which gives for $\Delta S°_{298}$ a value difficult to account for. In addition, the entropy change of reaction 1 was calculated using different methods, and the results were in satisfactory agreement (see Table 5). As a result, we can consider that our combined experimental and theoretical approach has provided reliable values of the thermochemical parameters for reaction 1. There are no direct measurements in the literature, but the enthalpy change of reaction 1 can be compared with the results of theoretical calculations

$$\Delta H°_0 = -71.1 \text{ kJ mol}^{-1} \quad \text{(Yu et al.)}[5]$$

$$\text{and} \quad \Delta H°_0 = -80.6 \text{ kJ mol}^{-1} \quad \text{(Glenewinkel-Meyer et al.)}[16]$$

to be compared to our value, derived from experimental measurements ($\Delta H°_0 = -83.8 \pm 8.0$ kJ mol^{-1}). The value of Glenewinkel-Meyer et al. agrees with our value within combined uncertainties whereas that of Yu et al. appears too low.

The bond dissociation energy (BDE) of phenoxy−NO is the lowest measured to date for a bond between a radical and NO. A few values are shown for comparison in Table 6. It is more than 80 kJ mol^{-1} smaller than BDE values generally observed

TABLE 6: Resonance Stabilization Energies and R−NO Bond Dissociation Energies for a Few Typical Radicals

R	RSE/kJ mol^{-1}	BDE(R−NO)/kJ mol^{-1}	ref
CH_3		172	(29)
t-C_4H_9		167	(30)
CF_3		167	(29)
CCl_3		125	(26)
$C_6H_5CH_2$	52.3[a]	123	(10)
CH_2CHCH_2	62.8[a]	110	(10)
C_6H_5O	83.7[b]	87	(this work)

[a] Reference 28. [b] Reference 27.

for alkyl and fluorinated alkyl radicals. The particular case of CCl_3 has already been discussed in previous publications.[10,25,26] This low BDE(phenoxy−NO) must be related to the strong resonance stabilization energy (RSE) that has been determined for the phenoxy radical, 83.7 kJ mol^{-1}.[27] It should be noted that the difference in BDEs for R−NO bonds between those of alkyl radicals and those of resonance-stabilized radicals, such as benzyl, allyl, and phenoxy, is very close to the RSE of the latter radicals, as shown in Table 6. In addition, note that the differences between BDEs are almost exactly the same as the difference in RSEs for these radicals.

The high resonance stabilization energy associated to the phenoxy radical must be related to the absence of reaction that was observed between this radical and O_2.[6] Because of this high RSE it is likely that this radical may not even form a stable peroxy radical (phenoxy−O_2).

Acknowledgment. The authors thank A. A. Boyd for his help in the preparation of the manuscript and the Ministry of Environment and the European Community (Copernicus Program) for financial support.

References and Notes

(1) Buth, R.; Hoyermann, K.; Seeba, J. *25th Symp. (Int. Combust.* **1994**, 841.

(2) He, Y. Z.; Mallard, W. G.; Tsang, W. *J. Phys. Chem.* **1988**, *92*, 2201.

(3) Mulcahy, M. F. R.; Williams, D. J. *Nature (London)* **1963**, *199*, 761.

(4) Mulcahy, M. F. R.; Williams, D. J. *Aust. J. Chem.* **1965**, *18*, 20.

(5) Yu, Y.; Mebel, M.; Lin, M. C. *J. Phys. Org. Chem.* **1995**, *8*, 47.

(6) Berho, F.; Lesclaux, R. *Chem. Phys. Lett.*, in press.

(7) Lightfoot, P. D.; Lesclaux, R.; Veyret, B. *J. Phys. Chem.* **1990**, *94*, 700.

(8) de More, W. B.; Sander, S. P.; Golden, D. M.; Molina, M. J.; Hampson, R. F.; Kurylo, M. J.; Howard, C. J.; Kolb, C. E.; Ravishankara, A. R. Chemical Kinetics and Photochemical Data for Use in Stratospheric Modeling. NASA−JPL Publication, 92-20, Pasadena, CA, 1990.

(9) Ye, M.; Schuler, R. H. *J. Phys. Chem.* **1989**, *93*, 1898.

(10) Boyd, A. A.; Nozière, B.; Lesclaux, R. *J. Phys. Chem.* **1995**, *99*, 10815.

(11) Becke, A. D. *J. Chem. Phys.* **1993**, *98*, 5648.

(12) Lee, C.; Yang, W.; Parr, R. G. *Phys. Rev.* **1988**, *B37*, 785.

(13) Frisch, M. J.; Trucks, G. W.; Schlegel, H. B.; Gill, P. M. W.; Johnson, B. G.; Robb, M. A.; Cheeseman, J. R.; Keith, T.; Peterson, G. A.; Montgomery, J. A.; Raghavachari, K.; Al-Laham, M. A.; Zakrzewski, V. G.; Ortiz, J. V.; Foresman, J. B.; Cioslowski, J.; Stefanov, B. B.; Nanayakkara, A.; Challacombe, M.; Peng, C. Y.; Ayala, P. Y.; Chen, W.; Wong, M. W.; Andres, J. L.; Replogle, E. S.; Gomberts, R.; Martin, R. L.; Fox, D. J.; Binkley, J. S.; Defrees, D. J.; Baker, J.; Stewart, J. P.; Head-Gordon, M.; Gonzales, C.; Pople, J. A. *GAUSSIAN 94*, Revision C.2; Gaussian, Inc.: Pittsburgh, PA, 1995.

(14) Qin, Y.; Wheeler, R. A. *J. Chem. Phys.* **1995**, *102* (4), 1689.

(15) Qin, Y.; Wheeler, R. A. *J. Am. Chem. Soc.* **1995**, *117*, 6083.

(16) Glenewinkel-Meyer, T.; Crim, F. F. *J. Mol. Struct.: THEOCHEM* **1995**, *337*, 209.

(17) Tripathi, G. N. R.; Schuler, R. H. *J. Chem. Phys.* **1984**, *81*, 113.

(18) Tripathi, G. N. R.; Schuler, R. H. *J. Phys. Chem.* **1988**, *92*, 5129.

(19) Dewar, M. J. S.; Thiel, W. *J. Am. Chem. Soc.* **1977**, *99*, 4899.

(20) AMPAC 5.2, 1994, Semichem**, 7128 Summit, Shawnee, KS, 66216.

(21) Chase, M. W., Jr.; Davies, C. A.; Downey, J. R., Jr.; Frurip, D. J.; McDonald, R. A.; Syveruid, A. N. *J. Phys. Chem. Ref. Data* **1985**, *14*, 1533.

(22) Lias, S. G.; Bartmess, J. E.; Liebman, J. F.; Holmes, J. L.; Levin, R. D.; Mallard, W. G. *J. Phys. Chem. Ref. Data* **1988**, *17*, 230.

(23) Baulch, D. L.; Cobos, C. J.; Cox, R. A.; Esser, C.; Frank, P.; Just, Th.; Kerr, J. A.; Pilling, M. J.; Troe, J.; Walker, R. W.; Warnatz, J. *J. Phys. Chem. Ref. Data* **1992**, *21*, 411.

(24) Dorthe, G. In *N-centered radicals*; Alfassi, Z., Ed.; John Wiley, to be published.

(25) Masanet, J.; Caralp, F.; Jemi-Alade, A. A.; Lightfoot, P. D.; Lesclaux, R.; Rayez, M.-T. *J. Phys. Chem.* **1993**, *97*, 3237.

(26) Ley, L.; Masanet, J.; Caralp, F.; Lesclaux, R. *J. Phys. Chem.* **1995**, *99*, 1953.

(27) Paul, S.; Back, M. H. *Can. J. Chem.* **1975**, *53*, 3330.

(28) Hrovat, D. A.; Borden, W. Y. *J. Phys. Chem.* **1994**, *98*, 10460.

(29) McCoustra, M. R. S.; Pfab, J. P. *Spectrochim. Acta* **1990**, *46A*, 937.

(30) Noble, M.; Quian, C. X. W.; Reisler, H.; Wittig, C. *J. Chem. Phys.* **1986**, *85*, 5763.